2017

Attaching the NorA Efflux Pump Inhibitor INF55 to Methylene Blue Enhances Antimicrobial Photodynamic Inactivation of Methicillin-Resistant Staphylococcus aureus in Vitro and in Vivo

Ardeshir Rineh
University of Wollongong, arineh@uow.edu.au

Naveen K. Dolla
University of Wollongong, nkd547@uowmail.edu.au

Anthony R. Ball
Gliese 623B

Maria Magana
Aeginition Hospital

John B. Bremner
University of Wollongong, jbremner@uow.edu.au

See next page for additional authors

Publication Details

Rineh, A., Dolla, N. K., Ball, A. R., Magana, M., Bremner, J. B., Hamblin, M. R., Tegos, G. P. & Kelso, M. J. (2017). Attaching the NorA Efflux Pump Inhibitor INF55 to Methylene Blue Enhances Antimicrobial Photodynamic Inactivation of Methicillin-Resistant Staphylococcus aureus in Vitro and in Vivo. ACS Infectious Diseases, 3 (10), 756-766.

Attaching the NorA Efflux Pump Inhibitor INF55 to Methylene Blue Enhances Antimicrobial Photodynamic Inactivation of Methicillin-Resistant Staphylococcus aureus in Vitro and in Vivo

Abstract
Antimicrobial photodynamic inactivation (aPDI) uses photosensitizers (PSs) and harmless visible light to generate reactive oxygen species (ROS) and kill microbes. Multidrug efflux systems can moderate the phototoxic effects of PSs by expelling the compounds from cells. We hypothesized that increasing intracellular concentrations of PSs by inhibiting efflux with a covalently attached efflux pump inhibitor (EPI) would enhance bacterial cell phototoxicity and reduce exposure of neighboring host cells to damaging ROS. In this study, we tested the hypothesis by linking NorA EPIs to methylene blue (MB) and examining the photoantimicrobial activity of the EPI-MB hybrids against the human pathogen methicillin-resistant *Staphylococcus aureus* (MRSA). Photochemical/photophysical and *in vitro* microbiological evaluation of 16 hybrids carrying four different NorA EPIs attached to MB via four linker types identified INF55-(Ac)en-MB 12 as a lead. Compound 12 showed increased uptake into *S. aureus* cells and enhanced aPDI activity and wound healing effects (relative to MB) in a murine model of an abrasion wound infected by MRSA. The study supports a new approach for treating localized multidrug-resistant MRSA infections and paves the way for wider exploration of the EPI-PS hybrid strategy in aPDI.

Disciplines
Medicine and Health Sciences

Publication Details
Rineh, A., Dolla, N. K., Ball, A. R., Magana, M., Bremner, J. B., Hamblin, M. R., Tegos, G. P. & Kelso, M. J. (2017). Attaching the NorA Efflux Pump Inhibitor INF55 to Methylene Blue Enhances Antimicrobial Photodynamic Inactivation of Methicillin-Resistant Staphylococcus aureus in Vitro and in Vivo. ACS Infectious Diseases, 3 (10), 756-766.

Authors
Ardeshir Rineh, Naveen K. Dolla, Anthony R. Ball, Maria Magana, John B. Bremner, Michael R. Hamblin, George P. Tegos, and Michael J. Kelso

Attaching the NorA Efflux Pump Inhibitor INF55 to Methylene Blue Enhances Antimicrobial Photodynamic Inactivation of Methicillin-Resistant *Staphylococcus aureus in vitro* and in *vivo*

Ardeshir Rineh,[†] Naveen K. Dolla,[†] Anthony R. Ball,[#] Maria Magana,[‡] John B. Bremner,[†] Michael R. Hamblin,[ϕ,¥,§] George P. Tegos,[#,*] Michael J. Kelso[†,*]

[†]Illawarra Health and Medical Research Institute and School of Chemistry, University of Wollongong, Northfields Ave., Wollongong, New South Wales, 2522, Australia.

[#]Gliese 623B, Lowell, MA 01852, USA.

[‡]Athens Medical School, Aeginition Hospital, Department of Biopathology and Clinical Microbiology, Athens, Greece.

[ϕ]The Wellman Center for Photomedicine, Massachusetts General Hospital, Boston, MA 02114, USA.

[¥]Department of Dermatology, Harvard Medical School, Boston, MA 02114, USA.

[§]Harvard-MIT Division of Health Sciences and Technology, Cambridge, MA 02114, USA.

*To whom correspondence should be addressed:

Illawarra Health and Medical Research Institute and School of Chemistry, University of Wollongong, Northfields Ave., Wollongong, New South Wales, 2522, Australia.

Phone: +61−2−4221 5085; Fax: +61 2 4221 4287

Email: mkelso@uow.edu.au

Gliese 623B, Lowell, MA 01852, USA.

Email: gtegos@gmail.com

ABSTRACT

Antimicrobial photodynamic inactivation (aPDI) uses photosensitizers (PSs) and harmless visible light to generate reactive oxygen species (ROS) and kill microbes. Multidrug efflux systems can moderate the phototoxic effects of PSs by expelling the compounds from cells. We hypothesized that increasing intracellular concentrations of PSs by inhibiting efflux with a covalently attached efflux pump inhibitor (EPI) would enhance bacterial cell phototoxicity and reduce exposure of neighbouring host cells to damaging ROS. In this study, we tested the hypothesis by linking NorA EPIs to methylene blue (MB) and examining the photoantimicrobial activity of the EPI-MB hybrids against the human pathogen methicillin-resistant *Staphylococcus aureus* (MRSA). Photochemical/photophysical and *in vitro* microbiological evaluation of sixteen hybrids carrying four different NorA EPIs attached to MB *via* four linker-types identified INF55-(Ac)en-MB **12** as a lead. Compound **12** showed increased uptake into *S. aureus* cells and enhanced aPDI activity and wound healing effects (relative to MB) in a murine model of an abrasion wound infected by MRSA. The study supports a new approach for treating localized multidrug-resistant MRSA infections and paves the way for wider exploration of the EPI-PS hybrid strategy in aPDI.

Keywords: antimicrobial photodynamic inactivation; photosensitizer-efflux pump inhibitor hybrid; methicilllin resistant *Staphylococcus aureus*; reactive oxygen species; bioluminescence wound infection model

Methicillin-resistant *Staphylococcus aureus* (MRSA) infections have emerged as a major medical threat over the past two decades.[1] Despite a downward mortality trend in Europe, MRSA remains a major cause of serious skin and soft-tissue infections,[2-4] community-acquired pneumonia and catheter-related bloodstream infections, and is responsible for the majority of recurrent infections in immunocompromised patients.[5] Several classes of antibiotics have been used to treat MRSA infections over the years, including the topically applied mupirocin, later generation β-lactams, broad spectrum tetracyclines, linezolid, the lipopeptide daptomycin, the glycopeptide vancomycin and the recently approved lipoglycopeptides telavancin, oritavancin and dalbavancin.[6] Some of these antibiotics have, or will likely become, ineffective against MRSA due to the development of resistance, thus ensuring an ongoing need for new antibiotics and treatment strategies targeting this significant human pathogen.[7]

Multidrug resistance often arises due to transmembrane efflux systems, which serve to pump noxious compounds from microbial cells.[8] Efflux systems in Gram-positive *cocci* (e.g. MRSA) tend to exhibit broad and overlapping substrate specificities, with many compounds (e.g. antibiotics, monovalent and divalent biocides, intercalating dyes, quaternary ammonium salts, diamidines, biguanidines and plant secondary metabolites) acting as efflux pump substrates.[9] Efflux-mediated resistance in *Staphylococci* has been attributed to pumps from the chromosomally encoded Major Facilitator Superfamily (MFS: NorA, NorB, NorC, MdeA),[10] the Multi-Antimicrobial Extrusion protein family (MATE: mepA),[10] Small Multidrug Resistance proteins (SMR: SepA)[11] and the plasmid encoded systems QacA, QacB and Tet(K).[12-14] The NorA pump has been extensively studied in *S. aureus*, including as a discovery target for small molecule efflux pump inhibitors (EPIs).[15]

Photodynamic therapy (PDT) is a light-based technology that harnesses the combined power of visible or near-visible light and photosensitizers (PSs) to kill cells. PSs are typically

non-toxic, highly conjugated aromatic molecules that exert photodynamic activity through reactions with molecular oxygen.[16] Illumination with light of a suitable wavelength and reaction of the excited-state PSs with O_2 generates reactive oxygen species (ROS) (e.g. singlet oxygen $^1O_2$ and hydroxyl radicals •OH) that cause non-specific cell damage and death. While PDT has been widely explored in the treatment of cancer[17] and age-related macular degeneration,[18] antimicrobial photodynamic inactivation (aPDI) has only more recently emerged as a powerful sterilization technique and promising treatment for localized bacterial infections.[19] The phenothiazinium PSs methylene blue (MB) and toluidine blue O (TBO), for example, are used for photodynamic sterilization of blood products and aPDI oral cavity disinfection.[20-23]

Efflux pumps have been shown to moderate bacterial cell killing during aPDI with MB, apparently by lowering intracellular MB concentrations and associated (intracellular) ROS.[24] This suggested that combination approaches, where MB is co-administered with a small molecule efflux pump inhibitor (EPI), should potentiate aPDI by increasing intracellular MB and associated ROS, thus triggering more damaging intracellular photodynamic reactions. Additionally, better localization of PSs to the bacterial intracellular space would reduce the damaging effects of the ROS generated in solution on neighboring host cells at infection sites, which could aid wound healing. Studies by Tegos et al. demonstrated that combinations of NorA EPIs and MB (a well-characterised NorA substrate) show enhanced PDI of *S. aureus* relative to MB alone.[25]

We previously reported an efflux pump inhibitor-antibacterial hybrid strategy for addressing NorA efflux-mediated resistance in *S. aureus*. The prototype hybrid (SS14) containing berberine, a weak antibacterial natural product and NorA substrate,[26, 27] covalently linked to the synthetic NorA EPI 5-nitro-2-phenylindole (INF55), showed potent antibacterial activity, rapidly accumulated in *S. aureus* cells and was more effective than co-administered

berberine/INF55 combinations in a *Caenorhabditis elegans* model of enterococcal infection.[28] Analogues of SS14 showed remarkably similar effects indicating that significant structural changes could be introduced into the hybrids without diminishing antibacterial action.[29, 30]

Phenothiazinium photosensitizers (e.g. MB) are amphipathic, planar, polycyclic aromatic cations and physicochemically similar to the quaternary ammonium aromatic alkaloid berberine. The structural and physicochemical similarities between berberine and MB, combined with the known susceptibility of both compounds to NorA-mediated efflux,[27] suggested that a NorA EPI-MB hybrid strategy might be successfully applied in aPDI of *S. aureus*. We hypothesized that the hydrophobic/cationic EPI-MB hybrids would, in a similar fashion to MB, spontaneously enter *S. aureus* cells due to the negative membrane potential.[31] Unlike MB, however, the hybrids would resist efflux due to the attached NorA EPI. The higher resulting intracellular hybrid concentrations would amplify intracellular ROS (following illumination) leading to enhanced lethality compared to MB, whose photodynamic reactions are restricted by efflux mostly to the cell exterior (Figure 1, Top). Importantly, EPI-MB hybrids would be more attractive for clinical development than PS/EPI inhibitor combinations due to the simpler scientific (i.e. active pharmaceutical ingredient/formulation optimization, administration and delivery) and regulatory approval pathway for single agent therapeutics.

This study aimed to test the hypothesis by: (1) identifying a lead EPI-MB hybrid that shows increased uptake into *S. aureus* cells and enhanced *in vitro* PDI of *S. aureus* relative to MB alone, and (2) demonstrating that the selected lead shows enhanced PDI activity (relative to MB) in a murine MRSA localized wound infection model. A focussed 16-member EPI-MB hybrid library was rationally designed and synthesised and its members systematically screened using photochemical, photophysical and *in vitro* microbiological assays with *S.*

aureus. Compound INF55(Ac)en-MB **12** emerged as the lead hybrid and was subsequently examined alongside MB for *in vivo* aPDI effects against MRSA. Experiments probing the mechanism of enhanced PDI activity with INF55(Ac)en-MB **12** were also explored.

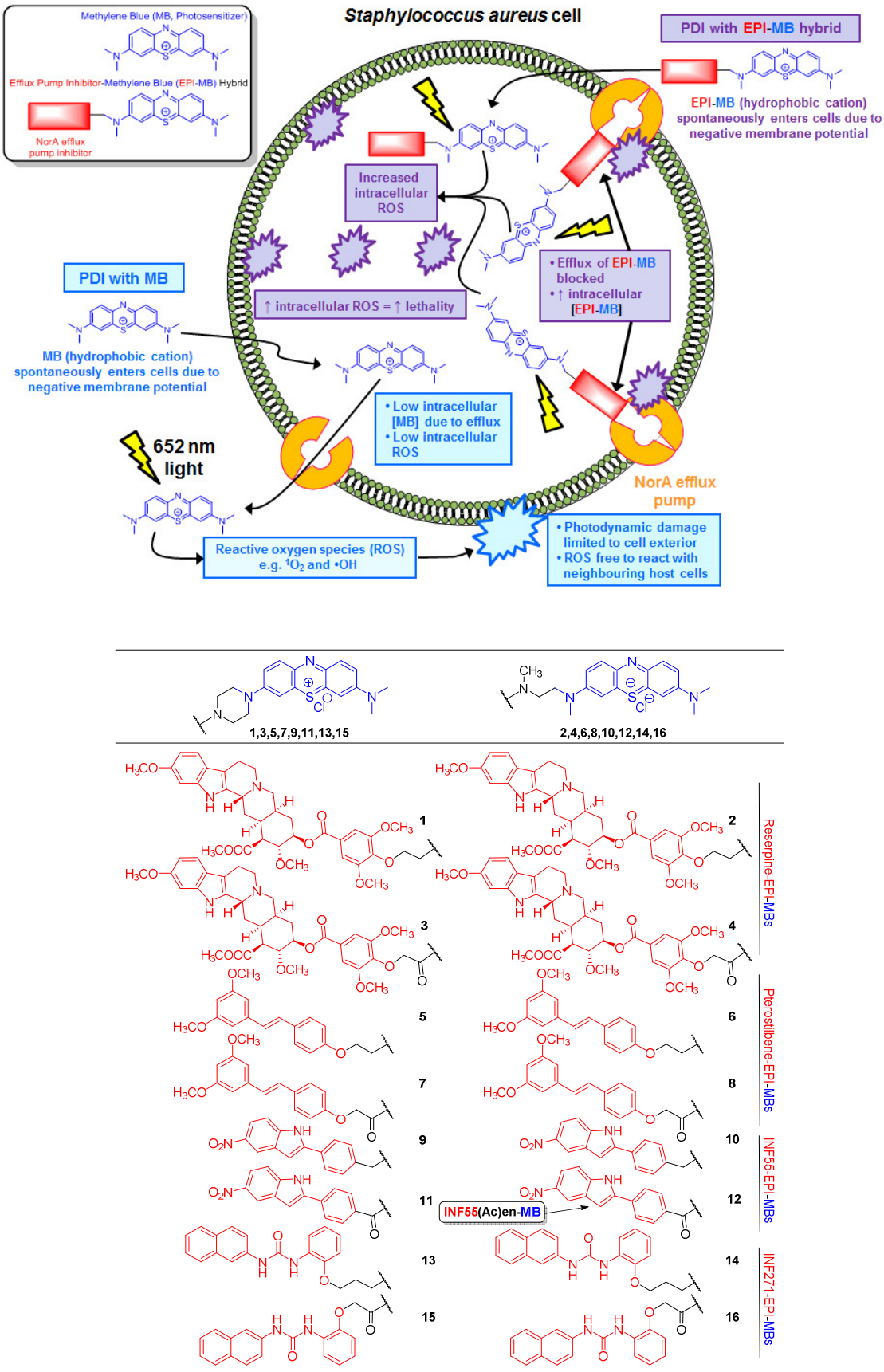

Figure 1. Proposed mechanism for enhanced PDI of *S. aureus* cells by EPI-MB hybrids relative to MB (Top). Structures of hybrids **1-16** (Bottom).

RESULTS AND DISCUSSSION

Library design and synthesis

At the outset of the study it was not known if linking NorA EPIs to MB would adversely impact EPI activities or the photochemical properties of MB. A medicinal chemistry approach was therefore adopted, where a focused library of 16 hybrids was synthesized with members containing four known NorA EPIs attached to MB *via* four different linker types. The structural variants were designed to systematically scan EPI-MB chemical space and increase the likelihood of identifying a lead hybrid for *in vivo* studies.

When designing EPI-MBs, we rationalized that only minimal structural modifications should be introduced at the phenothiazinium moiety in order to maintain the photosensitizer properties of MB. Such changes were considered less likely to impact ROS generation *via* the Type I (radical formation) and Type II (singlet oxygen formation) photochemical reactions of MB.[32] In the first compound series (**1**,**3**,**5**,**7**,**9**,**11**,**13**,**15**), the *N*-$(CH_3)_2$ group at the C-7 position of MB was replaced with a piperazine-based linker to direct EPIs away from the MB moiety. The second series (**2**,**4**,**6**,**8**,**10**,**12**,**14**,**16**) employed more flexible *N*,*N*'-dimethylethylenediamine-based linkers. Four *S. aureus* NorA efflux pump inhibitors (reserpine,[33] pterostilbene,[34] INF55[35] and INF271[35]) were appended to the linkers using both *N*-alkyl and *N*-acyl attachments as a way of systematically varying hybrid polarity and basicity. The structures of **1-16** are shown in Figure 1 (Bottom) and full details of their syntheses are provided in the Supporting Information, Section 1–Chemistry.

UV/Visible Spectroscopy

The absorption properties of the MB chromophore in hybrids **1-16** were probed using UV/visible spectroscopy. MB shows strong absorption bands between 550-700 nm, displaying an intense maximum at λ_{max1} = 668 nm and a shoulder at λ_{max2} = 609 nm.[36] Large

differences in wavelength and/or extinction coefficients at λ_{max1} and λ_{max2} for hybrids compared to MB would indicate that the structural modifications had altered the absorption properties of the chromophore. Hybrids exhibiting such changes were considered less likely to maintain the photosensitizer and aPDI properties of MB. UV/Visible spectra (Supporting Information, Supplementary Figure 5) and wavelength/extinction coefficient data (Supporting Information, Supplementary Figure 6) revealed that the λ_{max1} and λ_{max2} absorption bands varied little among MB and the hybrids, confirming that attachment of EPIs to MB had not significantly impacted the UV/visible absorption properties of the chromophore.

Photo-Induced $^1O_2$ and •OH Production by Hybrids

Effective aPDI with hybrids requires that sufficient ROS be produced from the compounds following illumination. Photo-induced $^1O_2$ and •OH production by hybrids **1-16** was examined by measuring the fluorescence emitted from co-dissolved ROS fluorescent reporter probes singlet oxygen sensor green (SOSG) and 3'-*p*-(hydroxyphenyl) fluorescein (HPF), respectively, following illumination with 652 nm red light. It has been shown that ROS generation by phenothiazinium PSs does not differ in the presence or absence of cells.[37] The $^1O_2$ and •OH data generated were thus relevant to the study's cell-based experiments (vide infra). Measurements for MB and hybrids **1-16** were performed in 96-well plates, plots of fluorescence versus light fluence generated (Supporting Information, Supplementary Figure 10) and the differences in fluorescence quantum yields relative to MB ($\%\Phi_\Delta$) were calculated (Figure 2).

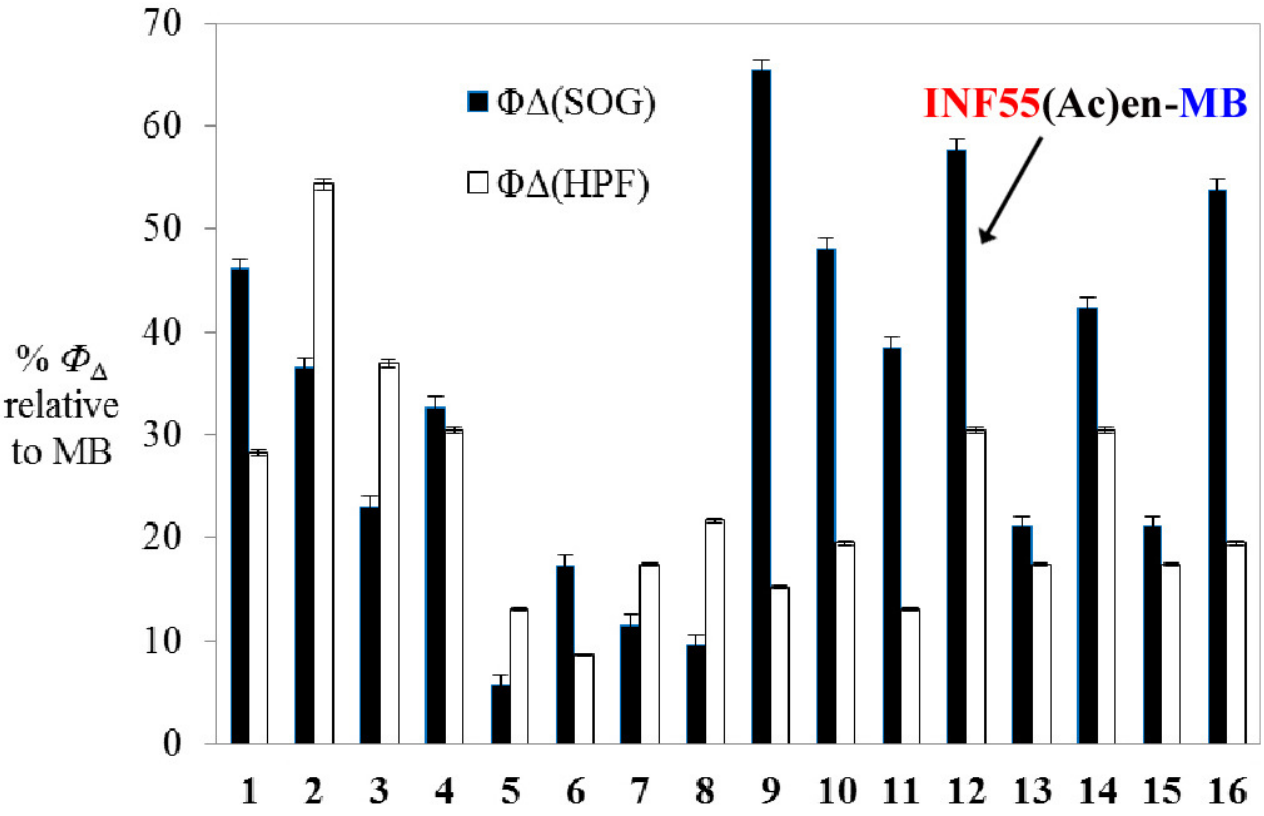

Figure 2. Fluorescence quantum yields (Φ_Δ) from SOSG ($^1O_2$) and HPF (•OH) probes following illumination of compounds **1-16** with 652 nm red light (0-12 J/cm^2). Data are reported as $\%\Phi_\Delta \pm$ SEM relative to MB from three independent experiments.

Generation of $^1O_2$ and •OH from all hybrids was lower than for MB. For reserpine-EPI-MBs **1-4** the levels ranged between 22-55% (of MB), while for Pterostilbene-EPI-MBs **5-8** the levels were less than 21%. INF55-EPI-MBs **9-12** and INF271-EPI-MB **16** showed greater than *ca* 2-fold higher $^1O_2$ production than •OH, with $^1O_2$ generation by **9** (65%) being the strongest of all the hybrids. Compound **12** (hereafter referred to as INF55(Ac)en-MB) generated the second highest $^1O_2$ levels (60%) and was the strongest producer of •OH (30%) among the INF55-EPI-MB series. Hybrid **16** from the INF271-EPI-MB series exhibited the third highest levels of $^1O_2$ production (55%).

In vitro PDI of MRSA USA300

For cell-based *in vitro* and *in vivo* experiments it was necessary to identify a non-toxic vehicle for solubilizing hybrids in aqueous media. Testing the aqueous solubility of reserpine-EPI-MB **3** (selected after noting its particularly poor aqueous solubility) using common detergents identified Cremophor EL® (CrEL) as a promising lead (Supporting Information, Supplementary Figure 11). CrEL was selected for use in all experiments after confirming it did not change photodynamic $^1O_2$ production by MB (relative to PBS/MeOH, Supporting Information, Supplementary Figure 10) and because of its reportedly low toxicity.[38]

Hybrids **1-16** were screened alongside MB for dose-dependent PDI of MRSA USA300 over the concentration range of 1-20 μM (652 nm red light, 6 J/cm^2). The complete data set is provided in the Supporting Information, Supplementary Figure 13. A summary of the activities observed at the highest concentration tested (20 μM) is shown in Figure 3. In dark control experiments, no significant toxicity was observed for any of the hybrids or MB and there was no difference between the dark toxicity of MB formulated in CrEL or PBS/MeOH (Supporting Information, Supplementary Figure 12). A 2 $\log_{10}$ reduction in survival was observed with MB (20 μM) in PBS upon light application, with an additional 1 $\log_{10}$ of killing seen when MB was formulated in CrEL. INF55(Ac)en-MB **12** showed the strongest aPDI activity, producing a 3 $\log_{10}$ greater killing effect than MB/CrEL at 20 μM. INF271-EPI-MBs **13** and **14** also showed higher activity than MB/CrEL, while reserpine-EPI-MB **4** and INF55-EPI-MB **10** produced equivalent killing effects (to MB/CrEL). The remaining hybrids all showed either lower or no activity.

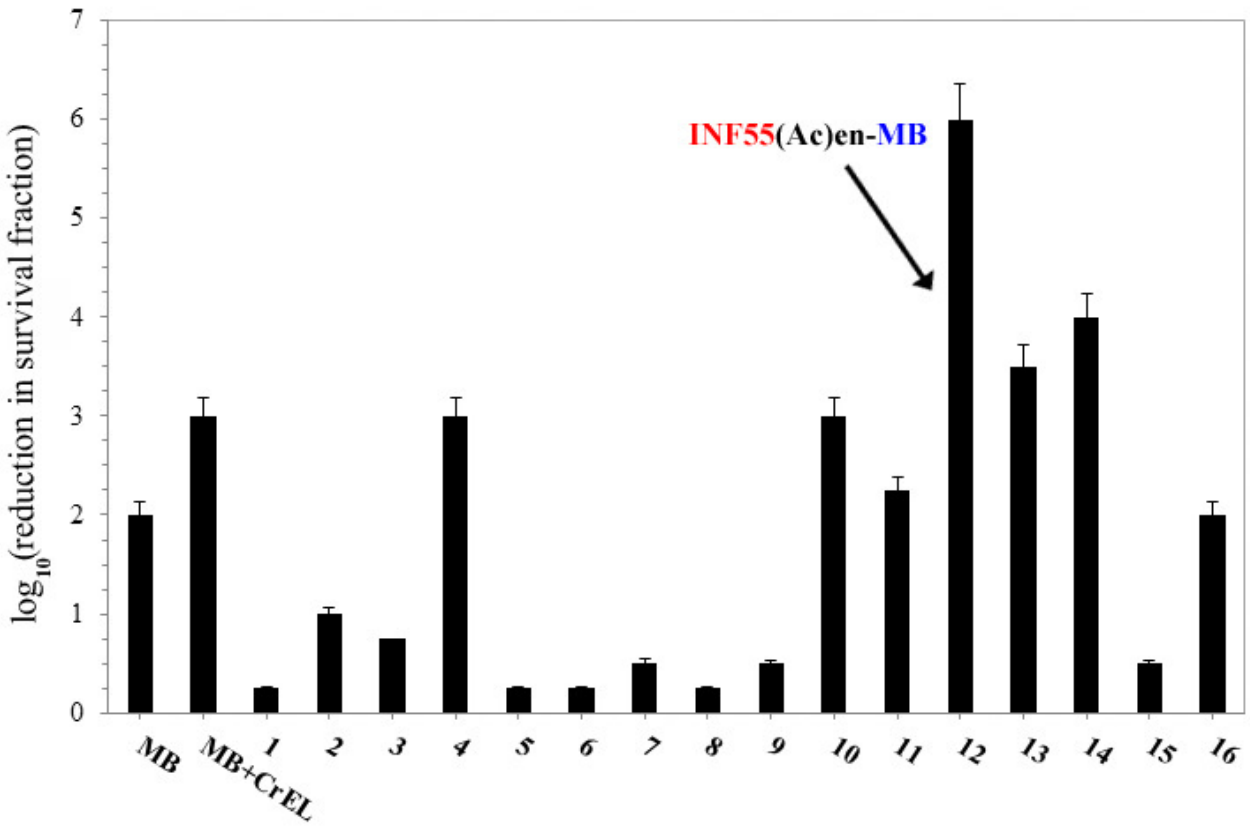

Figure 3. Photodynamic inactivation of MRSA USA300 by MB and hybrids **1-16** following illumination with 652 nm red light at 6 J/cm^2. All compounds were present at 20 μM. Data represent the mean of three independent experiments ± SEM.

PDI and uptake studies with *S. aureus* isogenic NorA efflux mutants

Previous studies with knockout (NorA-, K1758), wild-type (WT, 8325-4) and overexpressing (NorA++, K2361) *S. aureus* isogenic NorA efflux mutants showed that NorA expression correlates with reduced PDI by MB, due to the NorA-mediated efflux reducing intracellular MB concentrations and associated intracellular ROS.[25] Three hybrids exhibiting both significant ROS production and potent PDI of the MRSA USA300 strain (i.e. **10**, INF55(Ac)en-MB **12** and **14**) were selected for studies with the *S. aureus* NorA efflux mutants to examine the effects of this pump on hybrid PDI activity.

PDI of the *S. aureus* mutants was measured over the concentration range 0-160 μM at a constant light fluence. In dark control experiments, MB showed some dose-dependent toxicity at concentrations above 20 μM, especially against the NorA- and NorA++ strains. The hybrids were generally less toxic than MB at equivalent concentrations (Supporting Information, Supplementary Figure 14). Upon application of 652 nm red light (10 J/cm^2), MB (20 μM) caused a 2.9 $\log_{10}$ reduction in survival of the NorA- strain, and 2.2 $\log_{10}$ and 1.8 $\log_{10}$ reductions in the WT and NorA++ strains, respectively (Figure 4), in agreement with a previous report.[24]

The NorA++ strain showed a pronounced sensitivity to **10** and INF55(Ac)en-MB **12**, exhibiting an 8 $\log_{10}$ reduction in survival at concentrations above 40 μM. The NorA- strain also showed high sensitivity to INF55(Ac)en-MB **12**, while higher concentrations of **10** (80 μM) were required to produce an 8 $\log_{10}$ reduction in this strain. The three strains were uniformly less sensitive to the INF271-based hybrid **14**. The WT strain was the least sensitive towards all three hybrids at most concentrations.

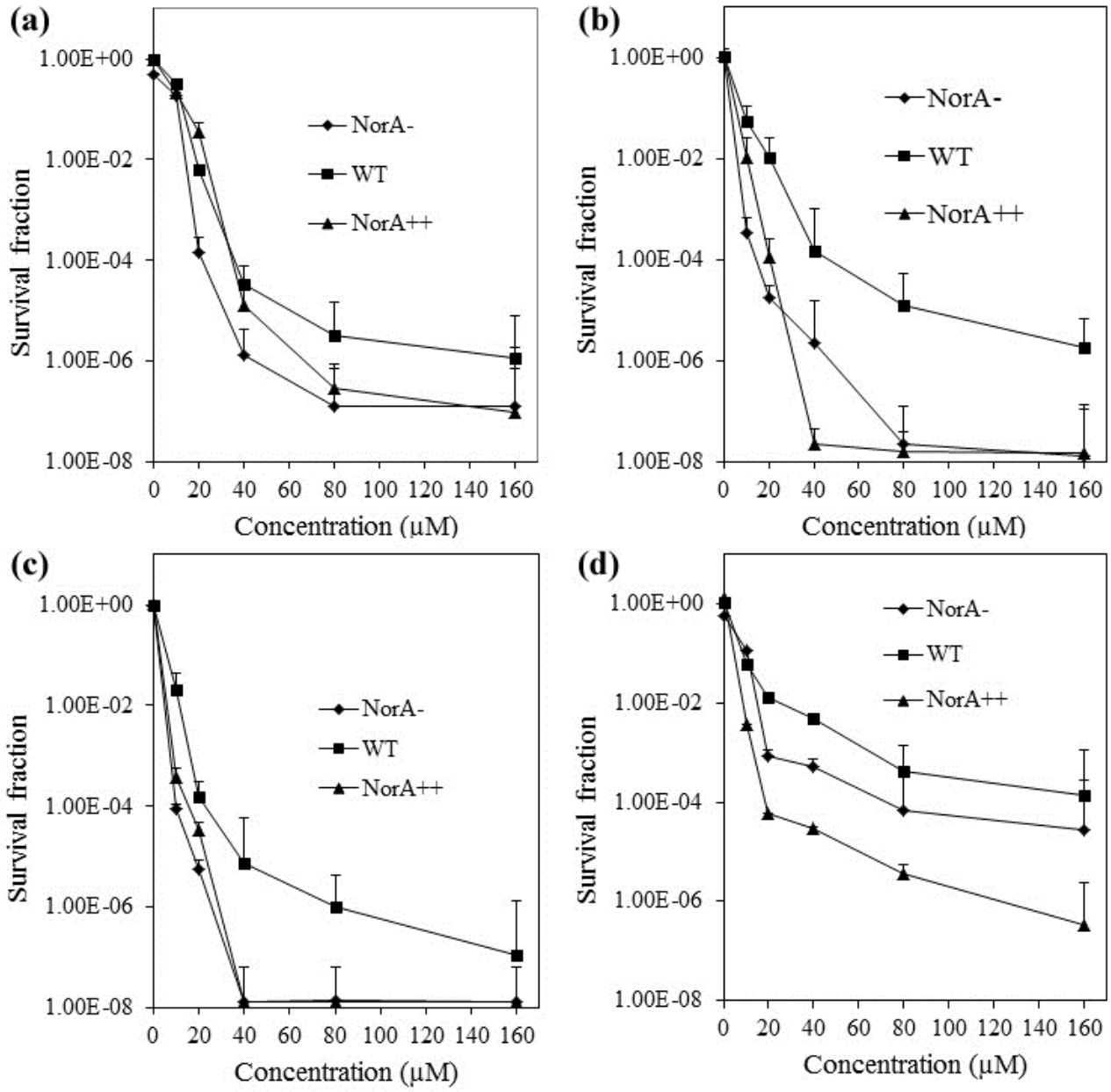

Figure 4. PDI of *S. aureus* NorA efflux mutants by: (a) MB, (b) **10**, (c) INF55(Ac)en-MB **12** and (d) **14** following illumination with 652 nm red light at 10 J/cm^2. Data represent the mean ± SEM from three independent experiments.

Cellular uptake of **10**, INF55(Ac)en-MB **12** and **14** by the three *S. aureus* NorA mutants was examined using a fluorescence-based assay. Uptake of MB was highest in the NorA- strain (3.7 x 10^9 molecules/cell), reduced in the WT (1 x 10^9 molecules/cell) and

lowest in the NorA++ strain (0.5 x 10^9 molecules/cell, Figure 5), consistent with susceptibility to NorA efflux.[25] Uptake of the three hybrids was similar and higher than MB in all strains. Hybrid uptake varied little among the strains despite the differences in NorA expression, suggesting that unlike MB the compounds are not susceptible to NorA efflux.

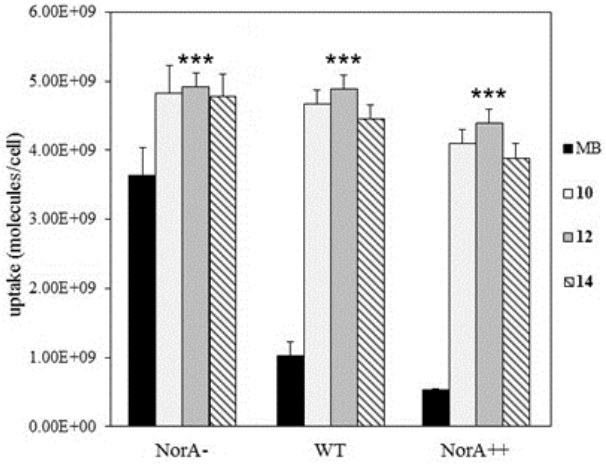

Figure 5. Uptake of MB and hybrids **10**, INF55(Ac)en-MB **12** and **14** by *S. aureus* isogenic NorA efflux mutants. All compounds were present at 20 μM. Data represent the mean ± SEM from three independent experiments. One-tailed *t* tests comparing MB uptake into each strain to uptake of each hybrid showed significant differences (***$P < 0.001$).

Inhibition of the NorA efflux pump

Having established that **10,** INF55(Ac)en-MB **12** and **14** accumulate in *S. aureus* cells and that they were not substrates for NorA, experiments were conducted to establish whether the hybrids also blocked the NorA pump. This was done by comparing PDI of NorA++ *S. aureus* cells by MB alone, MB in combination with the NorA EPIs INF55 and INF271 and MB in the presence of three hybrid surrogates, **30**, **31** and **32**. The surrogates corresponded to EPIs INF55 and INF271 functionalized with the (*N*-Boc-protected)-linker groups present in

10, **12** and **14**, respectively, with no MB attached (See Supporting Information, Section 1− Chemistry for the structures of **30-32**).

NorA++ *S. aureus* cells were treated with MB (20 μM) both alone and in combination with the EPIs (10 μM), illuminated with 652 nm red light (0-16 J/cm^2) and the survival fractions determined (Figure 6). For MB alone, a 2 $\log_{10}$ greater kill was observed at the maximum fluence (16 J/cm^2) compared to the dark control. In agreement with previous findings,[25] introduction of INF55 and INF271 potentiated MB PDI activity, affording an additional 4 $\log_{10}$ killing effect at 16 J/cm^2. PDI with MB in the presence of **30-32** was virtually unchanged from that observed with INF55 and INF271, confirming that the derivatized EPIs showed equivalent NorA inhibitory effects. Taken together, these results demonstrate that increased cellular uptake of **10**, INF55(Ac)en-MB **12** and **14** (relative to MB) into *S. aureus* cells arises from the direct inhibition of the NorA pump (by the appended EPIs) and not solely because the hybrids evade NorA-mediated efflux.

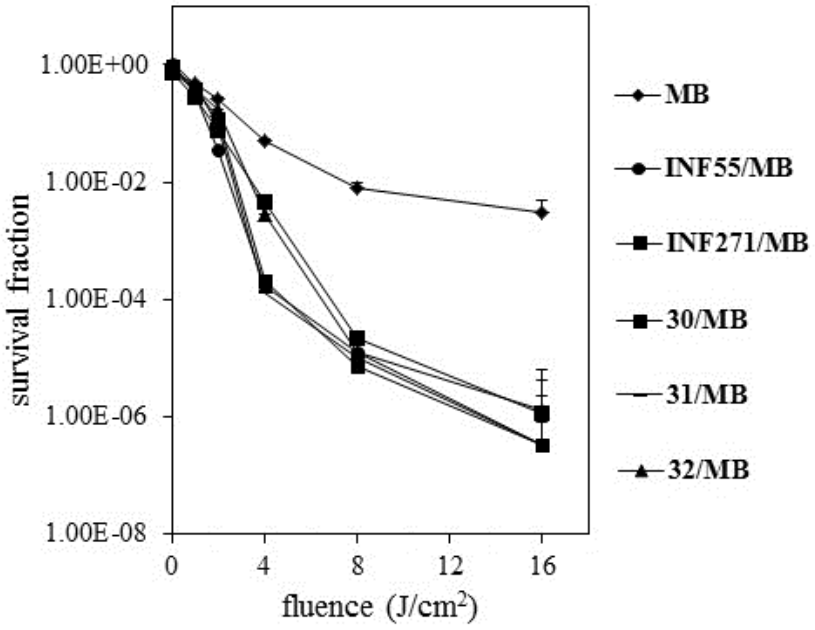

Figure 6. PDI of *S. aureus* NorA++ cells by MB (20 μM) and MB in combination with INF55, INF271 and derivatized EPIs **30-32** (all 10 μM). Data represent the mean ± SEM from three independent experiments.

Murine MRSA wound infection aPDI model

INF55(Ac)en-MB **12** was selected as the lead hybrid for *in vivo* studies where the goal was to establish whether the superior *S. aureus* cell uptake and *in vitro* PDI activity observed with **12** against MRSA relative to MB translated to increased efficacy in a whole-animal MRSA infection. Hybrid **12** was assessed alongside MB using the murine needle back-scratch wound abrasion aPDI model developed by Dai *et al*.[39] This model employs bioluminescent MRSA Xen30[40, 41] for facile infection monitoring and reflects the initial stages of the wound infection process.[39]

Immunosuppressed female BALB/c mice were divided into 5 cohorts, each containing 6 animals. Group A served as the negative control (no compound + light), Group B as the MB dark control (MB + no light) and Group C received MB + light. Group D served as the dark control for INF55(Ac)en-MB **12** (**12** + no light) and Group E received **12** + light. Back-

scratch wounds were introduced onto animals and inoculated with MRSA Xen30. Compound treatments were added by direct application to infection sites, red light (652 nm) was applied in 5 doses over 20 min and bioluminescence images were captured after each dose. A summary of the treatment cohorts and the experimental protocol is provided in the Supporting Information, Supplementary Figure 15. Representative images from animals in Groups A-E during the initial 'light-treatment' phase of the experiment are provided in the Supporting Information, Supplementary Figure 16. The quantitative wound bioluminescence data are presented in Figure 7(a).

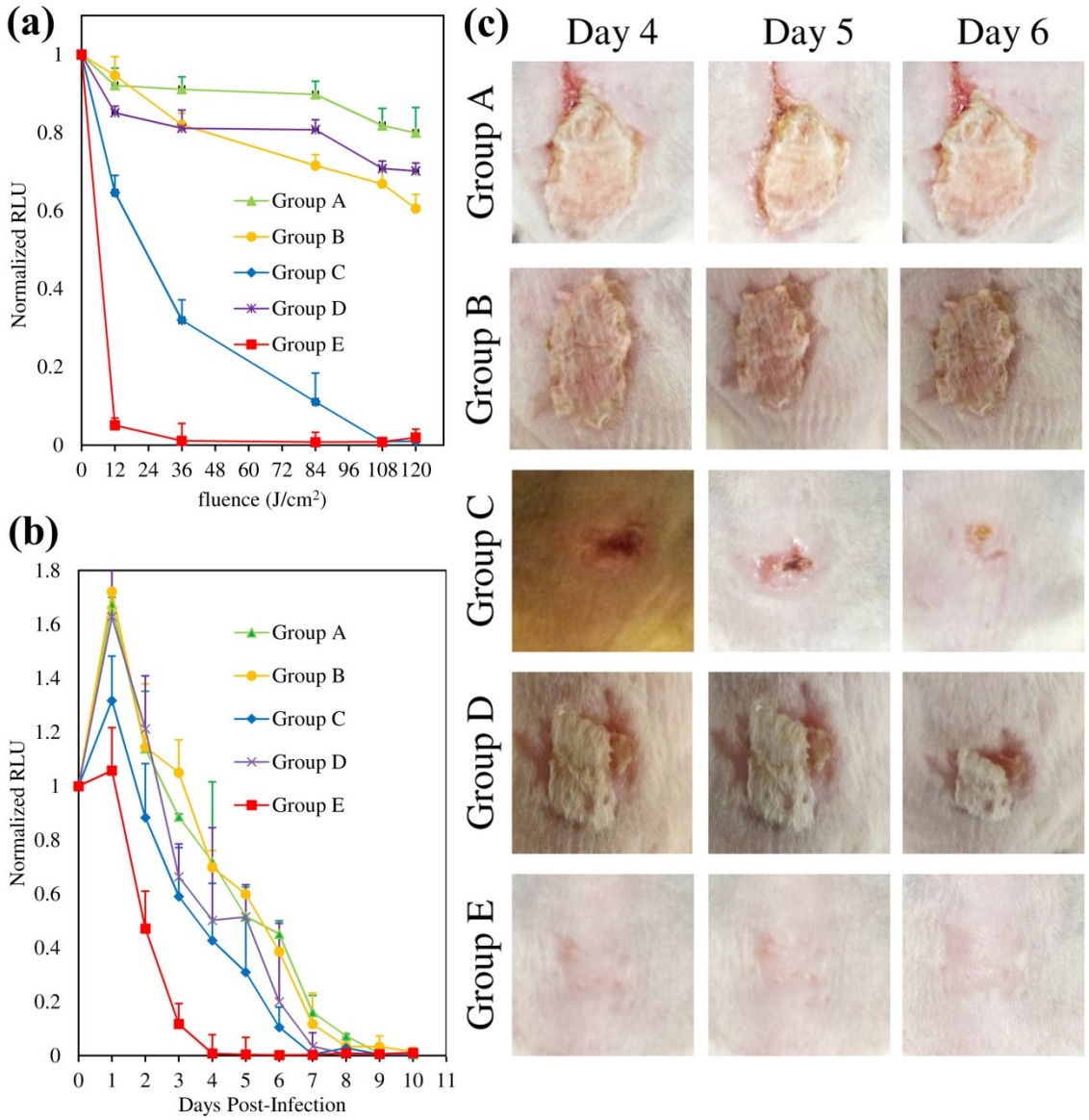

Figure 7. (a) Bioluminescence of MRSA Xen30-infected mouse wounds during initial 'light-treatment' phase. Data represent the mean (± SEM) normalized relative luminescence units (RLU) emanating from the wounds of 6 mice in each group. (b) Ten day post-treatment monitoring of infection site bioluminescence. Data represent the mean ± SEM (n = 6) for each cohort. (c) Photographs of infection sites in Groups A-E at Days 4-6 post-treatment.

In the absence of compound (Group A) the bioluminescence signal decreased less than 20%, confirming that the bacterial load was stable over the 20 min 'light-treatment' period. For the MB dark control (Group B) a 36% reduction in luminescence was observed.

Application of light to the MB–treated cohort (Group C) produced a light dose-dependent PDI response. After 2 min of light application (12 J/cm^2) bioluminescence was reduced by 45%, which increased to 70% after 6 min (36 J/cm^2) and became undetectable after 20 min (120 J/cm^2). For the INF55(Ac)en-MB **12** dark control (Group D) a 24% reduction in bioluminescence was seen after 20 min. A remarkable 98% reduction was observed with INF55(Ac)en-MB **12** after applying light for just 2 min (12 J/cm^2) and total loss of the bioluminescence signal was observed after 6 min.

Post-treatment monitoring of infection sites was performed for 10 days by capturing daily bioluminescence images (Supporting Information, Supplementary Figure 17). The bioluminescence signals were quantified and the data are presented in Figure 7(b). A rebound in the bacterial load, indicated by a ~1.6-fold increase in bioluminescence, was observed in the control groups (Group A, B and D) after Day 1 and their infections were resolved by Day 10. For the MB + light cohort (Group C), a smaller (1.3-fold) rebound was observed after 1 day and the infections were resolved within 7 days. For the INF55(Ac)en-MB **12** + light cohort (Group E), no rebound in the bacterial load was observed and the infections were completely resolved within 4 days. As shown in Figure 7(c), control Groups A, B and D exhibited minimal signs of healing on Days 4-6. The MB + light cohort (Group C) showed visible signs healing by Day 6, while animals treated with INF55(Ac)en-MB **12** + light (Group E) were healed by Day 4.

CONCLUSIONS

The need for continuous development of new therapeutic approaches targeting MRSA is high since: (i) the evolutionary adaptability of MRSA to antibiotic pressure has proven to be a remarkably successful survival strategy for this important human pathogen[42] and (ii) use of conventional broad spectrum antibiotics is a risk factor for increasing resistance, especially

in healthcare facilities.[43] Treatment of MRSA infections with antibiotics, including recently approved compounds[44] and new agents coming through the pipeline,[45] will likely afford only temporary solutions due to the inevitable development of resistance. In contrast, aPDI offers an attractive and easy-to-apply non-antibiotic alternative for treating localized MRSA infections that limits the development of resistance because of its multi-target/non-specific mode of action. aPDI approaches are predicted to have much longer effective clinical lifetimes than antibiotics.[46] In an era where there is an urgent need to identify anti-infective solutions beyond traditional antibiotics, aPDI offers extraordinary promise. Despite this, there have been surprisingly few clinical studies exploring aPDI[46-53].

This study explored the hypothesis that hybrid molecules, consisting of a NorA EPI covalently tethered to MB *via* a non-cleavable linker, could show increased aPDI activity relative to MB against MRSA. The hypothesis was founded on the idea that attaching the NorA EPI would increase intracellular concentrations of MB and associated intracellular ROS, leading to enhanced phototoxic effects. We predict that clinical use of such photoantimicrobials could provide effective aPDI treatments at low compound/light doses, thus reducing potential for ROS-mediated damage to host tissues. This is because concentrating ROS inside bacteria would place a protective (cell membrane) barrier between the phototoxic species and host cells. Preserving host tissues around infection sites should also provide benefits for wound healing through photobiomodulation effects.[54, 55]

UV/Visible absorption spectra of the 16 hybrids showed that the wavelengths and extinction coefficients of bands arising from the MB chromophore remained largely unchanged (relative to MB), indicating that the absorption properties of MB were not affected by the appended structures. INF55-EPI-MBs **10** and **12** and INF271 EPI-MBs **14** and **16** showed the strongest PDI of MRSA and uptake of **10**, **12** and **14** by the *S. aureus* NorA panel was much greater than MB and varied little across the phenotypes. Together these findings

indicated that EPI-MBs are not substrates for the NorA efflux pump. PDI experiments with MB in combination with INF55, INF271 and INF55- and INF271-containing compounds that lacked an appended MB group confirmed that these three hybrids also block the NorA pump.

The lead hybrid INF55(Ac)en-MB **12** was advanced to *in vivo* studies to establish whether its superior *in vitro* effects relative to MB translated to a vertebrate animal MRSA aPDI infection model. During the light treatment phase of the experiment INF55(Ac)en-MB **12** produced a more potent and rapid light-dose response than MB, while during the post-treatment monitoring period the bacterial re-growth observed with MB was not seen with **12**. More rapid clearance of bacteria was also observed and, crucially, wound healing occurred much earlier following treatment with INF55(Ac)en-MB **12** than MB.

This study demonstrates that attaching an EPI to a photosensitizer can increase aPDI efficacy, both *in vitro* and *in vivo*. The findings pave the way for pre-clinical assessment of aPDI with INF55(Ac)en-MB **12** in topical MRSA infections and support wider exploration of the EPI-PS approach as a method for treating drug resistant localized infections. As our fundamental understanding of microbial efflux pumps matures and our arsenal of EPI scaffolds expands, especially against Gram-negative pathogens, numerous opportunities will likely emerge for creating effective new EPI-PS hybrid photoantimicrobials.

METHODS

Chemistry. Complete details of the syntheses of hybrids **1**-**16** and all synthetic intermediates are provided in the Supporting Information, Section 1–Chemistry.

UV/Visible Spectroscopy. UV/Visible spectra were recorded over the wavelength range 250-750 nM using 10 μM solutions of MB and **1**-**16** in MeOH at 23 ^{o}C using a Shimadzu UV-1700 PharmaSpec Spectrophotometer spectrometer.

$^1O_2$ and •OH Experiments. Solutions of MB and hybrids **1**-**16** (50 μM, 85 μL) in phosphate-buffered saline (PBS, *p*H 11) were added to 96-well plates (Fisher Scientific, USA), followed by 40 μL of SOSG (5 μM) or HPF (5 μM) probes in PBS. D_2O (40 μL) was added to each well to increase the life-time of •OH and $^1O_2$[56, 57] and MeOH (40 μL) was added as co-solvent. Plates were illuminated with red light (652 nm) for times corresponding to 0-12 J/cm^2 fluence and plots of fluorescence versus fluence produced (Supporting Information, Supplementary Figure 10). A schematic summary of the experiments is provided in the Supporting information, Supplementary Figure 9.

A noncoherent light source (LC122; LumaCare, London, UK) with 30 nm-band-pass filters at ranges of 652 ± 15 nm was used for illumination. The total power output from the fibre bundle was 300 mW. Plates were arranged to give irradiance of 100 mW/cm^2. The power (P) in watts was equal to the energy (E) in joules, divided by the illumination time (t) in seconds:

$$P_{(W)} = E_{(J)} / t_{(s)}$$

So

$$\text{Watt/cm}^2 = \text{joule/cm}^2 \text{ per second}$$

A 30 sec illumination at irradiance 100 mW/cm^2 over a 3 cm^2 area provides a fluence of 1000 mJ/cm^2, or 1 J/cm^2. Fluence was proportionally increased by extending the period of illumination. A microplate spectrophotometer was used in "slow kinetic" mode for detecting fluorescence. For SOSG, emission was measured at 505 nm following excitation at 525 nm (2 nm monochromator band pass). For HPF, fluorescence emission was measured at 525 nm after excitation at 492 nm (2 nm monochromator band pass).

Fluorescence quantum yield is defined as the ratio of the number of photons emitted from a fluorophore to the number of photons absorbed. Relative fluorescence quantum yields in the SOG and HPF experiments were determined by comparing the observed fluorescence for hybrids **1**-**16** to MB, which produces known quantum yields under the experimental conditions (Φ_Δ SOG = 0.52, Φ_Δ HPF = 0.46). Quantum yields for the hybrids in each assay relative to MB were calculated using the equation:

$$\Phi_\Delta = \Phi_{\Delta MB} \times \frac{Int}{Int_{MB}} \times \frac{1\text{-}10^{-A_{MB}}}{1\text{-}10^{-A}} \times \frac{n^2}{n_{MB}^2}$$

Where *Int* is the area under the emission curve (on a wavelength scale), *A* is optical density at the excitation wavelength and *n* is the refractive index of the solvent. The subscript MB refers to the respective values for methylene blue. Since the same energies of light and the same solvents were used for MB and hybrids, the relative quantum yields could be obtained by measuring the area under the fluorescence curves (Supporting Information, Supplementary Figure 10) and dividing by the area under the MB curve. For each fluorescence curve, a best-fit trend line was obtained using polynomial regression and the relative integration calculated over the fluence range 0-10 J/cm^2 for SOG and 0-12 J/cm^2 for HPF. Further details regarding these experiments can be found in the Supporting Information, Section 3 – $^1O_2$ and •OH experiments.

Bacterial strains and culture conditions. Community Associated (CA)-MRSA (strain USA300, human isolate/Clinical Microbiology, Massachusetts General Hospital, MA, USA) was used for *in vitro* PDI screening of hybrids **1-16**. Mouse adapted *S. aureus* wild-type strain 8325-4 (Hamblin Lab), isogenic NorA efflux knockout strain (NorA-, SA-1758,

Hamblin Lab) and NorA overexpressing strain (NorA++, SA-K2378, Hamblin Lab)[58-60] were used for PDI and uptake studies with **10**, INF55(Ac)en-MB **12** and **14**. The bioluminescent MRSA Xen30 (LuxABCDE operon) strain used in the animal infection model was obtained from the Dai Lab, Wellman Center for Photomedicine, Massachusetts General Hospital, MA, USA.[40] Bacterial cells were cultured in Mueller–Hinton Broth (MHB) and growth was monitored using a Shimadzu Mini 1240 spectrometer at 600 nm (OD_{600}).

***In vitro* PDI studies with *S. aureus* MRSA USA300 and NorA efflux mutants.** MRSA USA300 cells (10^8 cfu/mL) were incubated with hybrids **1-16** or MB (0-20 μM) for 30 min at room temperature in 96-well plates before being illuminated with 652 nm light (6 J/cm^2). Wells were stirred constantly during illumination to ensure bacteria did not settle and were adequately mixed for sampling. Aliquots were removed, 10-fold serially diluted in PBS to provide 10^{-1} to 10^{-6} dilutions, streaked horizontally across square brain heart infusion agar plates and incubated overnight at 37 °C. Colony forming units were counted and survival fractions determined, as described by Jett *et al*.[61] Data are reported as $\log_{10}$ (reduction in survival fraction). Identical procedures were employed for PDI studies with **10**, INF55(Ac)en-MB **12** and **14** against the NorA isogenic mutants, except for use of 10 J/cm^2 fluence. For dark controls, the same procedures were used without the illumination step.

Cell uptake studies with *S. aureus* NorA efflux mutants. Uptake experiments were based on the procedure reported by Tegos *et al*.[25] Briefly, bacterial suspensions (10^8 cfu/mL) were incubated with compound (20 μM) in the dark at room temperature for 30 min. The cell suspensions were centrifuged (9,000 × *g*, 1 min) and the supernatant aspirated. The bacterial pellet was washed twice with sterile PBS (1 mL), centrifuged (9,000 × *g*, 1 min) and the

supernatant aspirated. The pellet was digested in 3 mL of 0.1 M NaOH containing 1% sodium dodecyl sulfate (SDS) for 48 h to give a homogenous solution. Fluorescence of the solution was measured using a spectrofluorimeter (FluoroMax3; SPEX Industries, Edison, NJ) with excitation at 650 nm and emission over the range 655-720 nm. Fluorescence calibration curves were generated from serial dilutions of each compound in 0.1 M NaOH/1% SDS. If necessary, cell digest solutions were diluted with 0.1 M NaOH/1% SDS until fluorescence fell within the linear region of the calibration curve. Cellular uptake was calculated by dividing the amount of compound (nmol) in the dissolved pellet by the number of cfu obtained from serial dilutions and converting to molecules/cell using Avogadro's number.

NorA efflux pump inhibition studies. Compounds **30** and **31**, corresponding to the (Boc-protected) INF55-linker groups found in **10** and **12**, respectively, and **32**, corresponding to the (Boc-protected) INF271-linker region in **14**, were intermediates in the synthesis of the parent hybrids (Supporting Information, Section 1–Chemistry). NorA++ *S. aureus* cells were incubated for 30 min at room temperature with INF55, INF271, **10**, **12** or **14** (all 10 μM) and MB (20 μM) in 96-well plates before illumination with increasing fluences of 652 nm red light (0-16 J/cm^2). Aliquots were removed and the survival fractions determined, as described above for the *in vitro* PDI studies.

Murine MRSA wound infection model. All procedures were approved by the Subcommittee on Research Animal Care at the Massachusetts General Hospital (MA, USA) and were in accordance with the guidelines of the National Institutes of Health (NIH). Stocks of MB and INF55(Ac)en-MB **12** were freshly prepared as CrEL/PBS micellar solutions to final concentrations of 200 μM (Supporting Information, Section 4(b) Preparation of CrEL

micellar solutions). Bioluminescent MRSA Xen30[40] cultures were grown overnight in brain heart infusion (BHI) media at 37 °C with 100 rpm orbital shaking. Bacterial growth was assessed using an Evolution 300 UV/Vis Spectrophotometer (Thermo Scientific, Waltham, MA, USA). Cultures of 0.8 optical density at 600 nm (OD_{600}) corresponded to 10^8 cfu/mL. Cells were washed with PBS, re-suspended in PBS to a density of 10^8 cfu/mL and used for wound inoculations.

Adult 7-8 week old female BALB/c mice weighing 17-21 g (Charles River Laboratories, Wilmington, MA, USA) were housed one per cage with access to food and water *ad libitum* while being maintained on a 12-hour light-dark cycle at 21 °C (relative humidity range 30-70%). Mice were immunosuppressed with intraperitoneal (i.p.) cyclophosphamide injections[62] 4 days (150 mg/kg i.p.) and 1 day (100 mg/kg i.p.) prior to MRSA Xen30 inoculation. On the day of inoculation, mice were anesthetized with i.p. injections of ketamine (100 mg/kg)/xylazine (10mg/kg) cocktail and their dorsal surfaces shaved. Skin abrasion wounds were introduced onto the dorsal surfaces by using a 28-gauge needle (Micro-Fine IV, Becton Dickinson, Franklin Lakes, NJ) to scratch 6 x 6 cross-hatch lines in a square covering 1.0 cm^2. The scratches were applied such that only the stratum corneum and upper-layer of the epidermis were damaged. Five minutes after wounding a 40 µL aliquot was drawn from the 10^8 cfu/mL suspension of MRSA Xen 30 in PBS and spread evenly over the wound area using a micropipette. Bioluminescence images were captured immediately after inoculation. Thirty minutes after inoculation, MB and INF55(Ac)en-MB **12** (40 µL of 200 µM stock solutions) were introduced to infection sites on animals from Groups B-E using a micropipette and a second bioluminescence image was captured. Fifteen minutes after compound addition (to allow binding/penetration into cells) a third image was captured (Time = 0). Mice were then illuminated with 652 nm light in 2, 4, 8, 4 and 2 min aliquots over a 20 min period, corresponding to fluences of 12, 36, 84, 108 and 120 J/cm^2.

Bioluminescence images were captured after each light dose. For the negative control Group A and dark controls Groups B and D, images were captured at the equivalent times post-inoculation. Bioluminescence images were captured daily for 10 days following treatment to monitor clearance of the infection and daily photographs were taken (Nikon Coolpix L20 camera) to record wound healing.

A noncoherent light source (LC122; LumaCare, London, UK) with interchangeable fibre bundles and 30 nm band-pass filters (652 ± 15 nm) was used for light application. Power output from the fibre bundle was 300 mW, with spots positioned at the required distance from animals to give an irradiance of 100 mW over the 1.0 cm^2 wound area. Bioluminescence images were captured using a Hamamatsu Photonics KK (Bridgewater, NJ) imaging system,[39] consisting of an intensified charge-coupled-device (ICCD), camera (C2400-30H; Hamamatsu), camera controller, imaging box, image processor (C5510-50; Hamamatsu) and color monitor (PVM 1454Q; Hamamatsu). Mice were placed on an adjustable stage in the specimen chamber and infected areas positioned directly under the camera. Light-emitting diodes were mounted inside the imaging box to supply light for dimensional imaging. The setup allowed a grayscale background image of each mouse to be taken. Luminescence emanating from wounds was captured using an integration time of 2 min at the maximum setting on the image-intensifier control module. ARGUS software (Hamamatsu) was used to present luminescence as false-colour images (pink most intense, blue least intense) superimposed on the grayscale background and to calculate relative luminescence units (RLU) from total pixel values.

ASSOCIATED CONTENT

Supporting Information

The Supporting Information is available free of charge on the ACS Publications website at DOI: XXXXXXXX

Details of the synthesis and characterization of hybrids and all synthetic intermediates, UV/Visible spectroscopy data, $^1O_2$ and •OH assays, *in vitro* PDI screening data, supporting *in vivo* data and descriptions of experiments.

AUTHOR INFORMATION

Corresponding authors

*(George P. Tegos) E-mail: gtegos@gmail.com

*(Michael J. Kelso) E-mail: mkelso@uow.edu.au

ORCID

Michael Kelso: 0000-0001-7809-6637

Author contributions

A.R. completed the majority of the synthetic chemistry, all of the photophysical/photochemical measurements, *in vitro* microbiology and *in vivo* experiments and helped to draft the manuscript. N.K.D assisted in the synthesis of INF55-MB hybrids **9-12**. A.R.B. and M.M. helped in designing experiments and in manuscript preparation. J.B.B. advised on the synthesis of hybrids and provided critical feedback on the manuscript. M.R.H. and G.P.T. oversaw all non-synthetic chemistry experiments. G.P.T and M.J.K conceptualized, initiated and directed the project.

Notes

The authors declare no competing financial interests.

ACKNOWLEDGEMENTS

We thank the University of Wollongong (Wollongong, Australia) and Massachusetts General Hospital (Boston, USA) for supporting this work. The study was partially funded by the US NIH (R01 AI076372 to J.B.B and M.J.K; AI050875 to M.R.H). Professor Kim Lewis (Northeastern University, MA, USA) and Professor Frederick Ausubel (Harvard Medical School, MA, USA) are gratefully acknowledged for discussions that helped initiate this work.

ABBREVIATIONS

aPDI, antimicrobial photodynamic inactivation; PS, photosensitizer; reactive oxygen species, ROS; efflux pump inhibitor, EPI; methylene blue, MB; methicillin-resistant *Staphylococcus aureus,* MRSA; photodynamic therapy, PDT; 5-nitro-2-phenylindole, INF55; Cremophor EL®, CrEL; wild-type, WT.

REFERENCES

(1) Nimmo, G. R., USA300 abroad: global spread of a virulent strain of community-associated methicillin-resistant *Staphylococcus aureus*. *Clin. Microbiol. .Infec.* **2012,** *18*, 725-734. DOI: 10.1111/j.1469-0691.2012.03822.x

(2) Mediavilla, J. R.; Chen, L.; Mathema, B.; Kreiswirth, B. N., Global epidemiology of community-associated methicillin resistant *Staphylococcus aureus* (CA-MRSA). *Cur. Opin. Microbiol.* **2012**, *15*, 588-595. DOI: 10.1016/j.mib.2012.08.003

(3) Garcia-Migura, L.; Hendriksen, R. S.; Fraile, L.; Aarestrup, F. M., Antimicrobial resistance of zoonotic and commensal bacteria in Europe: the missing link between consumption and resistance in veterinary medicine. *Vet. Microbiol.* **2014**, *170*. DOI: 10.1016/j.vetmic.2014.01.013

(4) Moran , G. J.; Krishnadasan , A.; Gorwitz , R. J.; Fosheim , G. E.; McDougal , L. K.; Carey , R. B.; Talan , D. A., Methicillin-resistant *S. aureus* infections among patients in the emergency department. *N. Engl. J. Med.* **2006**, *355*, 666-674. DOI: 10.1056/NEJMoa055356

(5) Vyas, K.; Hospenthal, D. R.; Mende, K.; Crum-Cianflone, N. F., Recurrent community-acquired methicillin-resistant *Staphylococcus aureus* infections in an HIV-infected person. *J. Clin. Microbiol.* **2011**, *49*, 2047-53. DOI: 10.1128/JCM.02423-10

(6) Maria, M.; Anastasios, I.; Emmanouil, M.; Oleg, U.; Cristian, G. B.; Stylianos, C.; Michael, R. H.; George, P. T., Therapeutic options and emerging alternatives for multidrug

resistant staphylococcal infections. *Cur.t Pharm. Des.* **2015**, *21*, 2058-2072. DOI: 10.2174/1381612821666150310101851

(7) Karam, G.; Chastre, J.; Wilcox, M. H.; Vincent, J.-L., Antibiotic strategies in the era of multidrug resistance. *Crit. Care* **2016**, *20*, 136. DOI: 10.1186/s13054-016-1320-7

8. Alekshun, M. N.; Levy, S. B., Molecular mechanisms of antibacterial multidrug resistance. *Cell* **2007**, *128*, 1037-1050. DOI: 10.1016/j.cell.2007.03.004

(9) Blanco, P.; Hernando-Amado, S.; Reales-Calderon, J.; Corona, F.; Lira, F.; Alcalde-Rico, M.; Bernardini, A.; Sanchez, M.; Martinez, J., Bacterial multidrug efflux pumps: much more than antibiotic resistance determinants. *Microorganisms* **2016**, *4*, 14. DOI:10.3390/microorganisms4010014

(10) Costa, S. S.; Viveiros, M.; Amaral, L.; Couto, I., Multidrug efflux pumps in *Staphylococcus aureus*: an update. *Open Microbiol. J.* **2013**, *7*, 59-71. DOI: 10.2174/1874285801307010059

(11) Narui, K.; Noguchi, N.; Wakasugi, K.; Sasatsu, M., Cloning and characterization of a novel chromosomal drug efflux gene in *Staphylococcus aureus*. *Biol. Pharm. Bul.* **2002**, *25*, 1533-1536. DOI.org/10.1248/bpb.25.1533

(12) Brown, M. H.; Skurray, R. A., Staphylococcal multidrug efflux protein QacA. *J. Mol. microbiol. biotechnol.* **2001**, *3*, 163-70.

(13) Xu, Z.; O'Rourke, B. A.; Skurray, R. A.; Brown, M. H., Role of transmembrane segment 10 in efflux mediated by the staphylococcal multidrug transport protein QacA. *J. Biol. chem.* **2006**, *281*, 792-9. DOI: 10.1074/jbc.M508676200

(14) Jin, J.; Guffanti, A. A.; Bechhofer, D. H.; Krulwich, T. A., Tet(L) and tet(K) tetracycline-divalent metal/H+ antiporters: characterization of multiple catalytic modes and a mutagenesis approach to differences in their efflux substrate and coupling ion preferences. *J. Bacteriol.* **2002**, *184*, 4722-32. DOI: 10.1128/JB.184.17.4722-4732.2002

(15) Kourtesi, C.; Ball, A. R.; Huang, Y. Y.; Jachak, S. M.; Vera, D. M.; Khondkar, P.; Gibbons, S.; Hamblin, M. R.; Tegos, G. P., Microbial efflux systems and inhibitors: approaches to drug discovery and the challenge of clinical implementation. *Open Microbiol. J.* **2013**, *7*, 34-52. DOI: 10.2174/1874285801307010034

(16) Wainwright, M.; Byrne, M. N.; Gattrell, M. A., Phenothiazinium-based photobactericidal materials. *J. Photochem. Photobiol. B.* **2006**, *84*, 227-30. DOI: 10.1016/j.jphotobiol.2006.03.002

(17) Dolmans, D. E. J. G. J.; Fukumura, D.; Jain, R. K., Photodynamic therapy for cancer. *Nat. Rev. Cancer* **2003**, *3*, 380-387. DOI: 10.1038/nrc1071

(18) Newman, D. K., Photodynamic therapy: current role in the treatment of chorioretinal conditions. *Eye (London, England)* **2016**, *30*, 202-10. DOI: 10.1038/eye.2015.251

(19) St Denis, T. G.; Dai, T.; Izikson, L.; Astrakas, C.; Anderson, R. R.; Hamblin, M. R.; Tegos, G. P., All you need is light: antimicrobial photoinactivation as an evolving and emerging discovery strategy against infectious disease. *Virulence* **2011**, *2*, 509-20. DOI: 10.4161/viru.2.6.17889

(20) Floyd, R. A.; Schneider, J. E., Jr.; Dittmer, D. P., Methylene blue photoinactivation of RNA viruses. *Antiviral Res.* **2004**, *61*, 141-51. DOI: 10.1016/j.antiviral.2003.11.004

(21) Moreira, M. S.; de FreitasArchilla, J. R.; Lascala, C. A.; Ramalho, K. M.; Gutknecht, N.; Marques, M. M., Post-treatment apical periodontitis successfully treated with antimicrobial photodynamic therapy via sinus tract and laser phototherapy: report of two cases. *Photomed. Laser Surg.* **2015**, *33*, 524-8. DOI: 10.1089/pho.2015.3936

(22) Alsterholm, M.; Karami, N.; Faergemann, J., Antimicrobial activity of topical skin pharmaceuticals - an in vitro study. *Acta Derm. Venereol.* **2010**, *90*, 239-45. DOI: 10.2340/00015555-0840

(23) Wainwright, M., Methylene blue derivatives - suitable photoantimicrobials for blood product disinfection? *Int. J. Antimicrob. Agents* **2000**, *16*, 381-94. DOI: org/10.1016/S0924-8579(00)00207-7

(24) Tegos, G. P.; Masago, K.; Aziz, F.; Higginbotham, A.; Stermitz, F. R.; Hamblin, M. R., Inhibitors of bacterial multidrug efflux pumps potentiate antimicrobial photoinactivation. *Antimicrob. Agents Chemother.* **2008**, *52*, 3202-3209. DOI: 10.1128/AAC.00006-08

(25) Tegos, G. P.; Hamblin, M. R., Phenothiazinium antimicrobial photosensitizers are substrates of bacterial multidrug resistance pumps. *Antimicrob. Agents Chemother.* **2006**, *50*, 196-203. DOI: 10.1128/AAC.50.1.196-203.2006

(26) Tegos, G.; Stermitz, F. R.; Lomovskaya, O.; Lewis, K., Multidrug pump inhibitors uncover remarkable activity of plant antimicrobials. *Antimicrob. Agents Chemother.* **2002**, *46*, 3133-41. DOI: 10.1128/AAC.46.10.3133-3141.2002

(27) Stermitz, F. R.; Lorenz, P.; Tawara, J. N.; Zenewicz, L. A.; Lewis, K., Synergy in a medicinal plant: antimicrobial action of berberine potentiated by 5'-methoxyhydnocarpin, a multidrug pump inhibitor. *Proc. Natl. Acad. Sci. USA* **2000**, *97*, 1433-7. DOI: 10.1073/pnas.030540597

(28) Ball, A. R.; Casadei, G.; Samosorn, S.; Bremner, J. B.; Ausubel, F. M.; Moy, T. I.; Lewis, K., Conjugating berberine to a multidrug resistance pump inhibitor creates an effective antimicrobial. *ACS Chem. Biol.* **2006**, *1*, 594-600. DOI: 10.1021/cb600238x

(29) Samosorn, S.; Tanwirat, B.; Muhamad, N.; Casadei, G.; Tomkiewicz, D.; Lewis, K.; Suksamrarn, A.; Prammananan, T.; Gornall, K. C.; Beck, J. L.; Bremner, J. B., Antibacterial activity of berberine-NorA pump inhibitor hybrids with a methylene ether linking group. *Bioorg. Med. Chem.* **2009**, *17*, 3866-72. DOI: 10.1016/j.bmc.2009.04.028

(30) Tomkiewicz, D.; Casadei, G.; Larkins-Ford, J.; Moy, T. I.; Garner, J.; Bremner, J. B.; Ausubel, F. M.; Lewis, K.; Kelso, M. J., Berberine-INF55 (5-nitro-2-phenylindole) hybrid antimicrobials: effects of varying the relative orientation of the berberine and INF55 components. *Antimicrob. Agents Chemother.* **2010**, *54*, 3219-24. DOI: 10.1128/AAC.01715-09

(31) Mates, S. M.; Eisenberg, E. S.; Mandel, L. J.; Patel, L.; Kaback, H. R.; Miller, M. H., Membrane potential and gentamicin uptake in *Staphylococcus aureus*. *Proc. Natl. Acad. Sci. USA* **1982**, *79*, 6693-7.

(32) Tardivo, J. P.; Del Giglio, A.; de Oliveira, C. S.; Gabrielli, D. S.; Junqueira, H. C.; Tada, D. B.; Severino, D.; de Fátima Turchiello, R.; Baptista, M. S., Methylene blue in photodynamic therapy: from basic mechanisms to clinical applications. *Photodiagnosis Photody. Ther.* **2005**, *2*, 175-191. DOI: org/10.1016/S1572-1000(05)00097-9

(33) Schindler, B. D.; Patel, D.; Seo, S. M.; Kaatz, G. W., Mutagenesis and modeling to predict structural and functional characteristics of the *Staphylococcus aureus* MepA multidrug efflux pump. *J. Bacteriol.* **2013**, *195*, 523-33. DOI: 10.1128/JB.01679-12

(34) Belofsky, G.; Percivill, D.; Lewis, K.; Tegos, G. P.; Ekart, J., Phenolic metabolites of dalea versicolor that enhance antibiotic activity against model pathogenic bacteria. *J.Nat. Prod.* **2004**, *67*, 481-484. DOI: 10.1021/np030409c

(35) Markham, P. N.; Westhaus, E.; Klyachko, K.; Johnson, M. E.; Neyfakh, A. A., Multiple novel inhibitors of the NorA multidrug transporter of *Staphylococcus aureus*. *Antimicrob. Agents Chemother.* **1999**, *43*, 2404-8.

(36) Redmond, R. W.; Gamlin, J. N., A compilation of singlet oxygen yields from biologically relevant molecules. *Photochem. Photobiol.* **1999**, *70*, 391-475. DOI: 10.1111/j.1751-1097.1999.tb08240.x

(37) Price, M.; Reiners, J. J.; Santiago, A. M.; Kessel, D., Monitoring singlet oxygen and hydroxyl radical formation with fluorescent probes during photodynamic therapy. *Photochem. Photobiol.* **2009**, *85*, 1177-81. DOI: 10.1111/j.1751-1097.2009.00555.x

(38) Zhao, F. K.; Chuang, L. F.; Israel, M.; Chuang, R. Y., Cremophor EL, a widely used parenteral vehicle, is a potent inhibitor of protein kinase C. *Biochem. Biophys. Res. Commun.* **1989**, *159*, 1359-67. DOI: org/10.1016/0006-291X(89)92260-2

(39) Dai, T.; Tegos, G. P.; Zhiyentayev, T.; Mylonakis, E.; Hamblin, M. R., Photodynamic therapy for methicillin-resistant *Staphylococcus aureus* infection in a mouse skin abrasion model. *Lasers Surg. Med.* **2010**, *42*, 38-44. DOI: 10.1002/lsm.20887

(40) Ragàs, X.; Sánchez-García, D.; Ruiz-González, R.; Dai, T.; Agut, M.; Hamblin, M. R.; Nonell, S., Cationic porphycenes as potential photosensitizers for antimicrobial photodynamic therapy. *J. Med. Chem.* **2010**, *53*, 7796-7803. DOI: 10.1021/jm1009555

(41) Yeaman, M. R.; Filler, S. G.; Chaili, S.; Barr, K.; Wang, H.; Kupferwasser, D.; Hennessey, J. P.; Fu, Y.; Schmidt, C. S.; Edwards, J. E.; Xiong, Y. Q.; Ibrahim, A. S., Mechanisms of NDV-3 vaccine efficacy in MRSA skin versus invasive infection. *Proc. Natl. Acad. Sci. USA* **2014**, *111*, E5555-63. DOI: 10.1073/pnas.1415610111

(42) Hede, K., Antibiotic resistance: An infectious arms race. *Nature* **2014**, *509*, S2-3. DOI: 10.1038/509S2a

(43) Couderc, C.; Jolivet, S.; Thiebaut, A. C.; Ligier, C.; Remy, L.; Alvarez, A. S.; Lawrence, C.; Salomon, J.; Herrmann, J. L.; Guillemot, D., Fluoroquinolone use is a risk factor for methicillin-resistant *Staphylococcus aureus* acquisition in long-term care facilities: a nested case-case-control study. *Clin. Infect. Dis.* **2014**, *59*, 206-15. DOI: 10.1093/cid/ciu236

(44) Boucher , H. W.; Wilcox , M.; Talbot , G. H.; Puttagunta , S.; Das , A. F.; Dunne , M. W., Once-weekly dalbavancin versus daily conventional therapy for skin infection. *N. Engl. J. Med.* **2014**, *370*, 2169-2179. DOI: 10.1056/NEJMoa1310480

(45) Kurosu, M.; Siricilla, S.; Mitachi, K., Advances in MRSA drug discovery: where are we and where do we need to be? *Expert Opin. Drug Discov.* **2013**, *8*, 1095-116. DOI: 10.1517/17460441.2013.807246

(46) Wainwright, M., Photodynamic antimicrobial chemotherapy (PACT). *J. Antimicrob. Chemother.* **1998**, *42*, 13-28.

(47) Bryce, E.; Wong, T.; Roscoe, D.; Forrester, L.; Masri, B., A novel immediate pre-operative decolonization strategy reduces surgical site infections. *Antimicrob. Resist. Infec. Control* **2013**, *2*, O10. DOI: org/10.1186/2047-2994-2-S1-O10.

(48) Bassetti, M.; Schar, D.; Wicki, B.; Eick, S.; Ramseier, C. A.; Arweiler, N. B.; Sculean, A.; Salvi, G. E., Anti-infective therapy of peri-implantitis with adjunctive local drug delivery or photodynamic therapy: 12-month outcomes of a randomized controlled clinical trial. *Clin. Oral Implants Res.* **2014**, *25*, 279-87. DOI: 10.1111/clr.12155. Epub 2013 Apr 8.

(49) Kolbe, M. F.; Ribeiro, F. V.; Luchesi, V. H.; Casarin, R. C.; Sallum, E. A.; Nociti, F. H., Jr.; Ambrosano, G. M.; Cirano, F. R.; Pimentel, S. P.; Casati, M. Z., Photodynamic therapy during supportive periodontal care: clinical, microbiologic, immunoinflammatory, and patient-centered performance in a split-mouth randomized clinical trial. *J. periodontol.* **2014**, *85*, e277-86. DOI: 10.1902/jop.2014.130559.

(50) Lopes, R. G.; de Godoy, C. H.; Deana, A. M.; de Santi, M. E.; Prates, R. A.; Franca, C. M.; Fernandes, K. P.; Mesquita-Ferrari, R. A.; Bussadori, S. K., Photodynamic therapy as a novel treatment for halitosis in adolescents: study protocol for a randomized controlled trial. *Trials* **2014**, *15*, 443. DOI: 10.1186/1745-6215-15-443.

(51) Figueiredo Souza, L. W.; Souza, S. V.; Botelho, A. C., Randomized controlled trial comparing photodynamic therapy based on methylene blue dye and fluconazole for toenail onychomycosis. *Dermatol. Ther.* **2014**, *27*, 43-7. DOI: 10.1111/dth.12042.

(52) Morley, S.; Griffiths, J.; Philips, G.; Moseley, H.; O'Grady, C.; Mellish, K.; Lankester, C. L.; Faris, B.; Young, R. J.; Brown, S. B.; Rhodes, L. E., Phase IIa randomized, placebo-controlled study of antimicrobial photodynamic therapy in bacterially colonized, chronic leg ulcers and diabetic foot ulcers: a new approach to antimicrobial therapy. *Br. J. Dermatol.* **2013**, *168*, 617-24. DOI: 10.1111/bjd.12098.

(53) Brown, S., Clinical antimicrobial photodynamic therapy: phase II studies in chronic wounds. *J. Natl. Compr. Canc. Netw. JNCCN* **2012**, *10 Suppl 2*, S80-3. DOI: 10.6004/jnccn.2012.0182.

(54) Avci, P.; Gupta, A.; Sadasivam, M.; Vecchio, D.; Pam, Z.; Pam, N.; Hamblin, M. R., Low-level laser (light) therapy (LLLT) in skin: stimulating, healing, restoring. *Semin. Cutan. Med. Surg.* **2013**, *32*, 41-52.

(55) Sellera, F. P.; Sabino, C. P.; Ribeiro, M. S.; Gargano, R. G.; Benites, N. R.; Melville, P. A.; Pogliani, F. C., *In vitro* photoinactivation of bovine mastitis related pathogens. *Photodiagnosis Photodyn. Ther.* **2016**, *13*, 276-81. DOI: 10.1016/j.pdpdt.2015.08.007

(56) Ogilby, P. R.; Foote, C. S., Chemistry of singlet oxygen. 34. Unexpected solvent deuterium isotope effects on the lifetime of singlet molecular oxygen ($^1\Delta_g$). *J. Am. Chem. Soc.* **1981**, *103*, 1219-1221. DOI: 10.1021/ja00395a041

(57) Merkel, P. B.; Kearns, D. R., Remarkable solvent effects on the lifetime of $^1\Delta_g$ oxygen. *J. Am. Chem. Soc.* **1972**, *94*, 1029-1030. DOI: 10.1021/ja00758a071

(58) Sabatini, S.; Kaatz, G. W.; Rossolini, G. M.; Brandini, D.; Fravolini, A., From phenothiazine to 3-Phenyl-1,4-benzothiazine derivatives as inhibitors of the *Staphylococcus aureus* NorA multidrug efflux pump. *J. Med. Chem.* **2008**, *51*, 4321-4330. DOI: 10.1021/jm701623q

(59) Sabatini, S.; Gosetto, F.; Manfroni, G.; Tabarrini, O.; Kaatz, G. W.; Patel, D.; Cecchetti, V., Evolution from a natural flavones nucleus to obtain 2-(4-Propoxyphenyl)quinoline derivatives as potent inhibitors of the *S. aureus* NorA efflux pump. *J. Med. Chem.* **2011**, *54*, 5722-36. DOI: 10.1021/jm200370y

(60) Augustin, J.; Rosenstein, R.; Wieland, B.; Schneider, U.; Schnell, N.; Engelke, G.; Entian, K. D.; Gotz, F., Genetic analysis of epidermin biosynthetic genes and epidermin-negative mutants of staphylococcus epidermidis. *Eur. J. Biochem.* **1992**, *204*, 1149-54. DOI: 10.1111/j.1432-1033.1992.tb16740.x

(61) Jett, B. D.; Hatter, K. L.; Huycke, M. M.; Gilmore, M. S., Simplified agar plate method for quantifying viable bacteria. *BioTechniques* **1997**, *23*, 648-50.

(62) Vecchio, D.; Dai, T.; Huang, L.; Fantetti, L.; Roncucci, G.; Hamblin, M. R., Antimicrobial photodynamic therapy with RLP068 kills methicillin-resistant *Staphylococcus aureus* and improves wound healing in a mouse model of infected skin abrasion PDT with RLP068/Cl in infected mouse skin abrasion. *J. Biophotonics* **2013**, *6*, 733-742. DOI: 10.1002/jbio.201200121

For Table of Contents Use Only